

shared with *A. spicatum*. This striking difference in phosphorus acquisition occurred in zones where there was an abundance of actively absorbing roots of both shrub and grass. These results indicate that *A. desertorum* has a great capacity to obtain phosphate at the expense of *Artemisia*, even though the shrub has invested as much in root length and mycorrhizal associations in the interspaces with *A. desertorum* as in the interspaces shared with *A. spicatum*. This provides evidence of competitive exploitation as a mechanism of interspecific competition.

These findings also have implications for agricultural intercropping systems. Analogous experiments could provide important information on the competitiveness of different crop species for phosphate and the effectiveness of phosphate fertilization patterns.

References and Notes

- J. L. Harper, *Population Biology of Plants* (Academic Press, New York, 1977); J. R. Ehleringer, *Oecologia* **63**, 153 (1984); R. Robberecht *et al.*, *ibid.* **60**, 21 (1983); P. J. Fonteyn and B. E. Mahall, *Nature (London)* **275**, 544 (1978).
- W. G. Braakhekke, *Agric. Res. Rep. No. 902* (Center for Agrobiological Research, Wageningen, Netherlands, 1980).
- Recent taxonomic revisions make *A. spicatum* synonymous with *Pseudoroegneria spicata* (Pursh) Löve [A. Löve, *Taxon* **29**, 163 (1980)]. In evenly spaced mixed plantings of *Artemisia* with single species of *Agropyron* in the same area, *Artemisia* had a mean shoot biomass of 191 ± 32 g (95 percent confidence interval) when growing with *A. spicatum* and only 79 ± 20 g when growing with *A. desertorum* within 3 years of planting of uniform-sized shrubs and grasses. The proportion of *Artemisia* plants that were able to flower and produce seed was nearly ten times greater in plots with *A. spicatum* than in plots with *A. desertorum* (75 versus 8 percent of the population, respectively) 4 years after planting. Correspondingly, the root system of *Artemisia* was less extensive when it was planted with *A. desertorum* than with *A. spicatum* (4).
- M. M. Caldwell *et al.*, *Oecologia* **50**, 14 (1981); M. M. Caldwell and J. H. Richards, in *On the Economy of Plant Form and Function*, T. J. Givnish and R. H. Robichaux, Eds. (Cambridge Univ. Press, Cambridge, in press).
- P. H. Nye and P. B. Tinker, *Solute Movement in the Soil-Root System* (Univ. of California Press, Berkeley, 1977).
- Labeling with dual isotopes of phosphorus has been used in other applications [N. E. Christians, K. J. Karnok, T. J. Logan, *Commun. Soil Sci. Plant Anal.* **12**, 765 (1981); J. Shierlaw and A. M. Alston, *Plant Soil* **77**, 15 (1984)].
- A solution of 0.02N HCl (250 ml) containing 500 μ Ci of 32 P- or 33 P-labeled orthophosphoric acid was injected in a series of ten 30-cm-deep holes each spaced 2.5 cm apart in moist soil to approximate a plane of label midway between neighboring plants and normal to a line connecting the plant centers. The distribution of the two radioisotopes was randomized with respect to the grass species. The concentration of the added phosphorus was $<10^{-11}$ g/cm³, which is below that to which plants have been found to respond [M. K. Schenk and S. A. Barber, *Agron. J.* **71**, 921 (1979)].
- The concentration of exchangeable phosphorus in these soils is <6 ppm. Phosphorus desorption tests indicate 90 to 95 percent of added phosphorus is bound to these soils.
- The length of the experiment was limited by the short half-lives of the isotopes. The counts of the two isotopes were corrected for half-life, counting efficiency, and overlap of energies.
- The roots were removed from the soil by flotation, separated by species, and measured for length in an optical scanner. Only hand-separated roots of each species were measured, and many of the finest roots detached in flotation could not be identified as to species and were omitted.
- M. F. Allen, *Mycologia* **75**, 773 (1983). The number of mycorrhizal spores in interspace soil shared by *Artemisia* and *A. spicatum* or *A. desertorum* was 45 ± 16 or 63 ± 25 spores per gram of soil, respectively (means \pm standard deviations).
- N. Chiariello, J. C. Hickman, H. A. Mooney, *Science* **217**, 941 (1982); K. Ritz and E. I. Newman, *Oikos* **43**, 138 (1984).
- H. Thorgeirsson and J. H. Richards, *Bull. Ecol. Soc. Am.* **64**, 159 (1983).
- J. W. Radin and M. P. Eidenbock, *Plant Physiol.* **75**, 372 (1984).
- Roots of *A. desertorum* are thinner and root density tends to be greater than in *A. spicatum* (4).
- We thank R. F. Fisher, R. E. Wyse, and F. Smith for help and technical consultation and C. Busso and C. Tann for technical assistance. Supported by grant BSR-8207171 from the National Science Foundation and the Utah Agricultural Experiment Station.

15 February 1985; accepted 30 May 1985

The Crystallization of Ultralong Normal Paraffins: The Onset of Chain Folding

Abstract. *The nature of chain folding in polymers and the determination of the chain length at which folding occurs have been central questions in polymer science. The study of the formation of lamellar polymer crystals through chain folding has received a new impetus as a result of the recent synthesis of normal alkanes of strictly uniform chain lengths up to C₃₉₀H₇₈₂. Chain folding is found in all such paraffins starting with C₁₅₀H₃₀₂. As with polyethylenes obtained by conventional polymerization, the fold length in the normal alkanes varies with crystallization temperature, but it is always an integral reciprocal of the full chain length. This behavior indicates that the methyl end groups are located at the lamellar surface and that the fold itself must be sharp and adjacently reentrant.*

G. UNGAR

J. STEJNY

A. KELLER

*H. H. Wills Physics Laboratory,
University of Bristol,
Bristol BS8 1TL, United Kingdom*

I. BIDD

M. C. WHITING

*Department of Organic Chemistry,
University of Bristol*

One of the most remarkable characteristics of flexible polymers is that they crystallize by chain folding (1). There are still many questions about this general, yet largely unexplained, phenomenon and also controversial problems (2). Possibly one of the most intriguing questions concerns the transition from the traditional behavior of short-chain molecules to that of a typical polymer. More specifically, at what chain length does chain folding set in and what is the nature of this fold?

It is evident that the primary prerequisite for such an inquiry is the strict uniformity of the chain length in the material to be examined. Further, the chains must have end groups that are not "alien" to the system. Moreover, there should be sufficient background information on the crystallization behavior of the material, both in the oligomeric state and in the polymeric state. In past experiments (3-9), these conditions were never all satisfied simultaneously. As a consequence, conclusions such as could be reached were not sufficiently definitive or general to constitute a representative solution of the central problem.

Normal alkanes (*n*-alkanes) the oligomers of polyethylene, would be the best materials to examine, provided that sufficiently uniform preparations could be obtained with increasing chain lengths of up to several hundred carbon atoms. As a result of a new synthesis (10, 11), such materials have become available. The maximum length reached so far is C₃₉₀H₇₈₂, which should ensure overlap with polyethylenes obtained by conventional polymerization where chain folding is consistently observed.

We now report that *n*-alkanes with lengths as short as C₁₅₀H₃₀₂ are capable of crystallizing in a chain-folded manner. The fold lengths are integral reciprocals of the total chain lengths, and thus the chain ends must lie at the layer surfaces. The fold itself cannot contain more than a few chain members; hence it must be sharp and adjacently reentrant.

The *n*-alkanes used were prepared by the method of Bidd and Whiting (11) and had the following extended-chain melting points (T_m) as determined by differential scanning calorimetry (DSC) to an accuracy of 0.3 K: C₁₀₂H₂₀₆, $T_m = 388.9$ K; C₁₅₀H₃₀₂, $T_m = 396.4$ K; C₁₉₈H₃₉₈, $T_m = 399.8$ K; C₂₄₆H₄₉₄, $T_m = 401.8$ K; C₂₉₄H₅₉₀ (12), $T_m = 403.6$ K; and C₃₉₀H₇₈₂, $T_m = 405.2$ K. A comparison of T_m for our C₁₅₀H₃₀₂ with the data reported for the longest *n*-alkanes prepared in the past [394.2 K for C₁₄₀H₂₈₂ (13) and 395.4 K for C₁₆₀H₃₂₂ (14)] indicates a clear improvement in purity in our materials.

The samples were crystallized both from the melt and from solutions (Table

1). Three standard methods were used to examine the crystals (15): (i) low-frequency Raman spectroscopy, recording the longitudinal acoustic mode (LAM); (ii) small-angle x-ray scattering (SAX); and (iii) DSC.

LAM frequencies measure straight-chain length, L_{LAM} in terms of the vibration of a rod of length L_{LAM} as expressed by

$$\nu_1 = \frac{1}{2L_{LAM}} \left(\frac{E}{\rho} \right)^{1/2} \quad (1)$$

Here ν_1 is the frequency of the first-order mode, E is the longitudinal elastic modulus, and ρ is the density. SAX measures the average periodicity in a stack of layers formed by the chains, according to Bragg's law. This periodicity also includes the space taken up by the fold and any gaps between individual layers that could be affected by the mode of layer packing. DSC scans provide information on the melting behavior, which is closely related to the nature of chain folding.

All the samples provided prominent first-order LAM peaks, and in most cases higher orders were also observed. Representative examples are shown in Fig. 1.

The number of carbon atoms in the straight stems giving rise to the observed frequencies (n_{LAM}) and the ratios of n_{total} to n_{LAM} are listed in Table 1. The LAM frequencies (ν_1) correspond to straight-chain lengths that are very close either to those of the fully extended chains or to integral reciprocals thereof (Table 1). We conclude from these observations that (i) chain folding can be found in all n -alkanes with $n > 150$; (ii) chains fold in integral reciprocals of the extended chain length (within a limit of 5 percent in all cases); and (iii) the greater the supercooling during crystallization, the larger the number of folds per molecule, a feature that parallels the situation in crystalline polymers. As many as four folds per molecule (fold groups with five stems) were found in solution-crystallized $C_{390}H_{782}$.

Several orders of small-angle x-ray reflections were obtained from all samples. Because of the complexities of paraffin crystallography (16), we will present only the general scheme with some numerical examples. Two situations arise:

1) The SAX spacing (L_{SAX}) is very close to L_{LAM} , to within ~ 3 percent. For once-folded chain crystals of $C_{246}H_{484}$ rapidly cooled from the melt, L_{LAM} was 158 Å and L_{SAX} was 160 Å.

2) L_{SAX} is different from L_{LAM} . In such cases, L_{SAX} is always less than L_{LAM} . For crystals of $C_{246}H_{494}$ grown by

Table 1. Longitudinal acoustic mode frequencies (ν_1) and derived values for selected alkane samples.

n -Alkane chain	Mode of crystallization*	ν_1^+ (cm ⁻¹)	n_{LAM}^\ddagger	n_{total}/n_{LAM}	Suggested chain conformation
$C_{150}H_{302}$	From solution	16.4	152	0.99	
		32.0	78	1.93	
$C_{198}H_{398}$	From solution	25.6	97	2.04	
		37.9	66	3.01	
$C_{246}H_{494}$	From solution	30.8	81	3.04	
		38.(3)	65	3.8	
$C_{246}H_{494}$	Slowly cooled melt (0.7 K per minute)	10.0	249	0.99	
		20.0	124	1.98	
$C_{294}H_{590}$	Slowly cooled melt (0.2 K per minute)	8.0	311	0.95	
		16.3	153	1.93	
$C_{390}H_{782}$	From solution	32.5	77	5.09	
$C_{390}H_{782}$	Quenched melt	12.1	206	1.90	
		18.3	136	2.87	
$C_{390}H_{782}$	Slowly cooled melt (0.5 K per minute)	12.3	202	1.93	

*All solution crystallization at room temperature from petroleum ether. †First-order peak frequencies; spectra were recorded on a Coderg T800 triple monochromator instrument at 1-cm⁻¹ band pass with Ar⁺ laser 514.5-nm exciting radiation. ‡The relation $n_{LAM} = 3169/1.273 \nu_1$ was used (25).

cooling the melt more slowly than in the earlier case, L_{LAM} for the once-folded chain crystals was 158 Å but L_{SAX} was 129 Å. This finding implies that the chains are tilted to the basal layer surface. In this example, which is typical, the chains are inclined at 35° with respect

to the layer normal. Such a situation is familiar in the crystallography of paraffinoid substances, including chain-folded polyethylene. It corresponds to a staggered stacking of methyl groups or folds with the orthorhombic lattice within the layer interior otherwise preserved. Thus the basal plane will have a low index $\{hkl\}$ instead of $\{00l\}$ for the perpendicular structure. The 35° corresponds to a basal plane of $\{201\}$, a frequently occurring plane in paraffins (16) and polyethylene (17).

The DSC melting curves for these ultralong paraffins always consisted of discrete endotherms, either single or multiple. A representative thermogram is shown in Fig. 2a. The individual peaks could always be identified as due to the melting of extended-chain, once- or twice-folded chain crystals. The identification was substantiated by the information obtained from the Raman spectra and SAX patterns of the same material crystallized under the same conditions. However, the thin-layer crystals that formed at high supercooling refolded during the DSC scan. This behavior manifested itself by the appearance of either an endotherm-exotherm-endotherm sequence (see Fig. 2b) or, in the extreme cases of very unstable crystals, a small exotherm followed by the melting endotherm of the refolded or chain-extended form. This behavior was more marked when the rates of heating were low. As a rule, melting endotherms of the solution-grown, chain-folded crystals in their original form were not observed.

The thermal data suggest a threefold

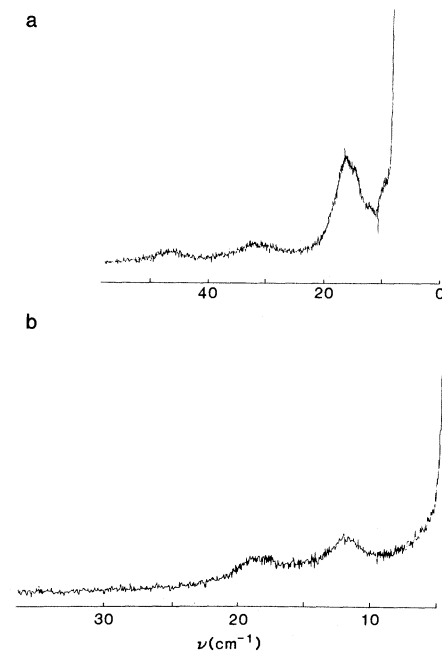


Fig. 1. (a) Low-frequency Raman spectrum of solution-crystallized n - $C_{150}H_{302}$ (peaks at 16 and 47 cm⁻¹ are due to the first- and third-order LAM's of the extended chains; the peak at 32 cm⁻¹ is due to the first-order mode of once-folded chains). (b) Low-frequency Raman spectrum of melt-quenched n - $C_{390}H_{782}$ (the lower and higher frequency peaks correspond to once- and twice-folded chains, respectively).

dependence of T_m : (i) on chain length [T_m is higher for longer chains (Table 1)]; (ii) on fold length (T_m is higher for longer folds for the same chain length); and (iii) on chain tilt in the case of chain-folded crystals.

The results obtained by all three experimental methods demonstrate the intrinsic tendency for chain-folded crystallization in linear molecules beyond a critical length. This length is not more than 150 carbon atoms, or 193 Å, in the case of polymethylene chains. The actual limiting value could be even lower. The tendency toward chain folding increases with increasing chain length. Folded chain crystals of $C_{150}H_{302}$ could be grown only at large supercoolings, either by solution crystallization or by melt quenching. Even then, they were mixed with the extended-chain form. In contrast, the longest paraffin, $C_{390}H_{782}$, tended to fold so readily that special measures had to be taken to obtain the extended form. Such measures involved prolonged isothermal crystallization at temperatures close to the melting point, for example, a 15-hour crystallization at 398.2 K, that is, at 7 K supercooling. Even this treatment produced only 62 percent (by weight) of the extended-chain form, the remainder being in the form of the once-folded crystals.

The lowest fold length obtained so far (L_{LAM} data) corresponds to 65 carbon atoms (85 Å) for solution-crystallized $C_{246}H_{494}$ (Table 1). Except for one special case (18), this value is markedly lower than usually encountered in polyethylene (19, 20).

The tendency of pure alkanes to fold in integral reciprocals of the extended chain length indicates the exclusion of chain ends from the crystal interior. In this way the impairment of lattice perfection through the presence of end groups is avoided. Such end-group exclusion modifies the lamellar thickness versus supercooling relation by making it a step function for any given paraffin instead of the continuous function normally observed in polydisperse macromolecular systems (1). Such a stepwise change in layer thickness has been observed by SAX measurements (6) and some remarkable optical microscopic studies (7, 8) of short polyethylene oxides which had narrow molecular weight distributions but were not monodisperse (21).

The analyses of Raman spectra can be used to examine the nature of the fold and fold surface. The ratios of n_{total} to n_{LAM} (Table 1) were very close to integral values, in all cases within 5 percent. Even the small departures were mainly in the direction corresponding to an

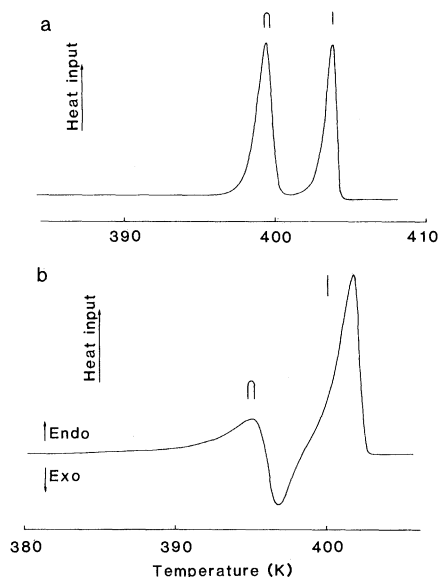


Fig. 2. (a) DSC thermogram of $n\text{-C}_{294}\text{H}_{590}$ slowly cooled from the melt (0.2 K/min); heating rate, 5 K/min. The two endotherms correspond to the melting of extended and once-folded chain crystals, as indicated. (b) DSC thermogram of melt-quenched $n\text{-C}_{246}\text{H}_{494}$ (heating rate, 10 K/min). Melting of once-folded chain crystals (low-temperature endotherm) is immediately followed by recrystallization (exotherm) in the extended-chain form, which melts at a somewhat higher temperature (high-temperature endotherm).

n_{LAM} larger than the appropriate integral reciprocal of the total carbon number in the chain. Hence it is unlikely that any appreciable portion of the chain is anywhere but in the straight stem, with only a small residual (say ~ 5 Å or so) set aside for an adjacent reentry fold when a fold is present. The data leave little leeway for the presence of a substantial fraction of longer folds, so it follows that the majority of folds must be sharp and adjacently reentrant. In fact, when L_{SAX} is compared with the corresponding calculated integral reciprocal of the extended chain length, the agreement is even closer; typically the difference does not exceed 2 to 4 Å.

The results of thermal analysis support the idea of chain folding and the discreteness of the fold-length values. They provide additional information on refolding to larger fold lengths when the paraffins are heated. Such behavior is characteristic of chain-folded systems, but in the present case refolding occurs in large discrete steps consistent with the LAM and SAX results. As a consequence, for the first time in a chain-folded system, net exotherms corresponding to an increase in fold length could also be identified.

Our results demonstrate the intrinsic tendency of these simple and unspecific chain molecules beyond a certain length

to fold on crystallization, and this in a sharply folded and adjacently reentrant manner. Accordingly, such behavior can be considered characteristic of the crystallization of long flexible chains in general. However, we do not wish to imply that all chains will behave exactly in the above fashion, irrespective of length. For increasingly longer chains crystallizing from the melt and particularly in polydisperse systems, the regular, adjacent, sharply folded deposition of chain segments will be increasingly disrupted by intervening neighboring molecules and by the trapping of remote parts of the same chain either through entanglements or by incorporation in other parts of the same crystal or in different crystals. Such effects will limit the extent of the adjacently reentrant, sharply folded sequence and create loose loops, hairs, and tie molecules. Such formations would be responsible for the amorphous characteristics of the fold surface and for much, if not all, of the amorphous content of an otherwise fully crystallized semicrystalline polymer. Yet the existence of such imperfections should not obscure the intrinsic trend of long chains to fold in a regular manner. Recent developments on biological polymers are fully consistent with this view. Neutron scattering and infrared spectroscopic studies on isotopically labeled materials (22–24) reveal clusters or subgroups of adjacent stems that originate in the same molecule but do not comprise the full molecule. We regard these subgroups as the long-chain equivalents of the chain-folded structures discussed here.

References and Notes

1. A. Keller, *Rep. Progress Phys.* **31**, 623 (1968).
2. *Faraday Discuss. Chem. Soc. No. 68* (1979).
3. A. Keller and A. O'Connor, *Polymer* **1**, 163 (1960).
4. H. Zahn and W. Pieper, *Kolloid Z. Z. Polym.* **180**, 97 (1962).
5. F. J. Balta-Calleja and A. Keller, *J. Polym. Sci. Part A 2*, 2151 (1963).
6. J. P. Arlie, P. Spegt, A. Skoulios, *Makromol. Chem.* **104**, 212 (1967).
7. A. J. Kovacs, A. Gonthier, C. Straupe, *J. Polym. Sci. Symp. No. 50* (1975), p. 283.
8. C. P. Buckley and A. J. Kovacs, in *Structure of Crystalline Polymers*, I. H. Hall, Ed. (Elsevier, New York, 1984), pp. 261–307.
9. A. Keller and Y. Udagawa, *J. Polym. Sci. Part A 2*, 221 (1972).
10. O. I. Paynter, D. J. Simmonds, M. C. Whiting, *Chem. Commun.* **1982**, 1165 (1982).
11. I. Bidd and M. C. Whiting, *ibid.* **1985**, 543 (1985).
12. The specimen contained ~ 8 percent of an accidental contaminant of lower molecular weight, probably $C_{198}H_{398}$, according to gel permeation chromatographic analysis.
13. W. Heitz *et al.*, *Makromol. Chem.* **162**, 63 (1972).
14. K. Takamizawa, Y. Ogawa, T. Oyama, *Polym. J.* **14**, 441 (1982).
15. A. Keller, in *Structural Order in Polymers*, F. Ciardelli and P. Giusti, Eds. (Pergamon, New York, 1980), p. 135.
16. W. Piesczek, G. R. Strobl, K. Malzahn, *Acta Crystallogr. Sect. B* **30**, 1278 (1974).
17. A. Keller and S. Sawada, *Makromol. Chem.* **74**, 190 (1964).
18. J. Martinez-Salazar, P. J. Barham, A. Keller, *J.*

- Polym. Sci. Polym. Phys. Ed.* **22**, 1085 (1984).
19. J. D. Hoffman, G. T. Davis, J. I. Lauritzen, in *Treatise on Solid State Chemistry*, N. B. Hannay, Ed. (Plenum, New York, 1976), vol. 3, chap. 7.
 20. R. A. Chivers *et al.*, *J. Polym. Sci. Polym. Phys. Ed.* **20**, 1717 (1982).
 21. Such results on polyethylene oxides are usually regarded as singularities in the polymer field rather than indicative of general behavior, particularly since other compounds, such as iodine-terminated polyethylenes of comparable polydispersity, did not display the quantized layer thickness effect (9). Nevertheless, a preference for chain ends to lie within the layer surface has been inferred even there, and also in short-chain polyethylenes with broad molecular-weight distributions [D. M. Sadler and A. Keller, *Kolloid Z. Z. Polym.* **242**, 1081 (1970)]. Our observations on *n*-alkanes are the more remarkable because the methyl end groups are closely similar to the

- chain members themselves. Nevertheless, the creation of vacancies when the methyl end groups are within the lattice or when they protrude from the layer appears sufficient to influence the fold length in the manner observed.
22. S. J. Spells and D. M. Sadler, *Polymer* **25**, 739 (1984).
 23. S. J. Spells, A. Keller, D. M. Sadler, *ibid.*, p. 749.
 24. S. J. Spells, *Polym. Commun.* **25**, 162 (1984).
 25. G. V. Fraser, *Ind. J. Pure Appl. Phys.* **16**, 344 (1978).
 26. We are indebted to P. Hendra for placing his Raman spectroscopic facility at our disposal when our own was not operational. G.U. and I.B. thank the Science and Engineering Research Council for financial support in the form of a research assistantship and a Ph.D. studentship, respectively.

26 December 1984; accepted 24 May 1985

Amino Acid Replacements That Compensate for a Large Polypeptide Deletion in an Enzyme

Abstract. *Deletion of more than 400 amino acids from the carboxyl terminus of an enzyme causes a severe reduction in catalytic activity. Selected point mutations within the residual protein partially reverse the effects of the missing segment. The selection can yield mutants with activities at least ten times as high as those of the starting polypeptides. One well-characterized mutation, a single amino acid replacement in the residual polypeptide, increases the catalytic activity of the polypeptide by a factor of 5. The results suggest substantial potential for design of protein elements to compensate for missing polypeptide sequences. They also may reflect that progenitors of large aminoacyl-tRNA (transfer RNA) synthetases—one of which was used in these studies—were themselves much smaller.*

CALVIN HO

MARIA JASIN

PAUL SCHIMMEL

*Department of Biology,
Massachusetts Institute of
Technology, Cambridge 02139*

We examined the possibility that a substantially truncated protein can require, through substitution of one or more amino acids some of the activity that is lost when a large polypeptide sequence is removed. Because there is no opportunity for compensatory interactions between mutant amino acids in the residual protein and the missing polypeptide sequences, the possibilities for restructuring the enzyme are limited.

There were two reasons for doing these studies. First, protein engineering is conceptually simpler and technically easier with small polypeptide chains. Many enzymes are large and, if they are to be redesigned or modified, the smallest possible unit of structure that retains activity is to be preferred. Removal of polypeptide sequences, however, can severely attenuate, if not eliminate, activity. This may pose constraints on how small an efficient enzyme for a particular reaction can be made.

The other reason concerns the overall design and organization of a particular class of enzymes, one member of which

was investigated in these studies. These are the aminoacyl-tRNA (transfer RNA) synthetases (1, 2). Some of these enzymes are large polypeptides (approximately 1000 amino acids), but there are data that support the hypothesis that the progenitors of these large enzymes were themselves much smaller (3, 4). The question is whether a barely active, small subfragment of a large synthetase has latent potential to retain specificity while reacquiring some of the catalytic activity that was lost on removal of a large segment of protein.

We demonstrated direct selection of a mutant fragment with enhanced catalytic activity. This was done without knowledge of the three-dimensional structure of the protein. The idea is that, for any strain construction in which the cell growth rate is severely retarded because of limited activity of the enzyme of interest, a mutant enzyme with enhanced specific activity will have accelerated growth and a clear selective advantage.

Mutagenesis and selection were applied to a catalytic fragment of *Escherichia coli* alanine tRNA synthetase. The enzyme catalyzes a two-step aminoacylation reaction of tRNA^{Ala}. The first reaction is synthesis of aminoacyl adenylate, which can occur in the absence of tRNA^{Ala}. The second reaction is between the enzyme-bound adenylate and

tRNA^{Ala}, to yield Ala-tRNA^{Ala}. The sum of the two reactions is the aminoacylation reaction.

The full-length enzyme is an 875-amino acid polypeptide (5). Aminoacylation of tRNA^{Ala} requires a 461-amino acid NH₂-terminal fragment, as judged by an *in vivo* complementation assay (3, 4). Although the activity is sufficient to achieve complementation of a specific mutation *in vivo*, the aminoacylation activity *in vitro* is virtually undetectable. There is no evidence for activity *in vivo* or *in vitro* for an amino-terminal fragment having 76 fewer amino acids (fragment of 385 *alaS* amino acids).

The original plasmid construction that encodes the 461 NH₂-terminal *alaS* codons specifies a polypeptide that complements the temperature-sensitive *alaS5* mutation but does not complement a strain that carries the Δ *alaS2* null allele (3, 4). This suggests that improving the specific activity of the fragment *in vivo* could result in complementation of the null allele background.

Plasmids pMJ385Nt and pCH461Nt, respectively, encode the 385- and 461-amino acid fragments at the NH₂-terminal of alanyl-tRNA synthetase, plus a COOH-terminal "tail" of 14 codons derived from pBR322. Plasmid pCH461Nt complements (at 42°C) the temperature-sensitive *alaS5* mutation (3). Plasmid pMJ385Nt complements neither *alaS5* nor Δ *alaS2* mutant alleles. The polypeptide encoded by pCH461Nt has low aminoacylation activity (see below). Although it is sufficient to complement the *alaS5* strain, it is insufficient for complementation of a specially constructed null allele, Δ *alaS2* (4, 6).

Heteroduplexes between these plasmids were formed and subjected to bisulfite mutagenesis (7, 8) (Fig. 1). (Except for the deleted nucleotides in pMJ385Nt and a removed Sal I site in pCH461Nt, the two plasmids are identical.) The mutagenized DNA was passed through a *ung*⁻ *alaS5* strain (9). This strain is temperature sensitive by virtue of the *alaS5* mutation; the uracil-*N*-glycosidase deficiency (*ung*⁻) assures that mutant uracils are not excised. The *ung*⁻ *alaS5* cells were also transformed with an untreated mixture of heteroduplex and linear DNA's. In this control experiment, about half of the transformants selected for plasmid-mediated ampicillin resistance (Amp^r) at the permissive temperature (30°C) were viable at the restrictive temperature (42°C). This established that segregation of the plasmids within the heteroduplex occurs after replication and that the deletion loop is retained in the 42°C transformants, because exci-